RUHUNA JOURNAL OF SCIENCE
Vol 10 (2): 120-134, Dec 2019
eISSN: 2536-8400
http://doi.org/10.4038/rjs.v10i2.78

Application of Lagrange equations to 2D double spring-pendulum in generalized coordinates

N.O. Nenuwe

Department of Physics, Federal University of Petroleum Resources, P. M. B. 1221, Effurun, Delta State, Nigeria, Nigeria

Correspondence: *nenuwe.nelson@fupre.edu.ng* https://orcid.org/0000-0002-3112-3869

Received: 31st December 2018; Revised: 30th July 2019; Accepted: 31st December 2019

Abstract In this study, the Lagrange's equations of motion for a 2D double spring-pendulum with a time dependent spring extension have been derived and solved approximately. The resulting equations are also solved numerically using Maple, and plots of motion for the pendulum bobs *m1* and *m2* are presented and compared. It was observed that motion along the x-axis is characterized by sine wave function while motion along y-axis is characterized by cosine wave function with slightly changing amplitudes. Change in stiffness constant, angle of deflection, mass of pendulum bob and spring length were found to have significant effect on the dynamics of the double spring-pendulum. The periodic and chaotic behaviour noticed in this study is consistent with current literature on spring-pendulum systems.

Keywords: Lagrange equations, double spring-pendulum.

1 Introduction

The two dimensional (2D) double pendulum is a typical example of chaotic motion in classical mechanics. The pattern of its motion is well known to change drastically as the energy is increased from zero to infinity (Biglari and Jami 2016). However, at low and very high energies the system represents coupled harmonic oscillators, and can be considered as an integrable system. But, at intermediate energies, the system is known to exhibit chaotic features.

Double spring-pendulum is a classical mechanical system consisting of two bobs of mass m_1 and m_2 fixed to the ends of two weightless elastic springs with stiffness constants k_1 and k_2, and the angle of deflections q_1 and q_2, respectively. The second spring is connected to the first mass as shown in Fig. 1.

The dynamics of double spring-pendulum appears to be scanty in literature, though there are reports on single and double spring pendulum systems. Marcus *et al.* (2016) studied the order-chaos-order transition of

spring pendulum using the Hamiltonian formulation. Numerical analysis of the equations of motion for double pendulum was reported by Smith (2002) using Maple soft. de Sousa *et al.* (2017) reported on the energy distribution in spring pendulum. Lewin *et al.* (2015) numerically analyzed the dynamics of single and double pendulum using MATLAB. Also, double pendulum numerical analysis with Lagrangian and Hamiltonian equations of motions using MATLAB was reported by Biglari and Jami (2016). Despite these studies, no reports to the best of my knowledge have been made on double spring-pendulum with time dependent extension in spring length using Lagrangian formulations.

Also, it is well known that physical systems can be described by their Lagrangian, and from the Lagrangian function one can obtain second order differential equations of motion describing such dynamic systems. In most cases the exact solution cannot be obtained for these Lagrange equations of motion, and this leads to employing alternative numerical approach to solve such equations (Baleanu *et al.* 2015).

The interest in this study is to analytically obtain the equations of motion for a double spring-pendulum with time dependent spring-extension. Hence, Lagrangian formulation of mechanics is used to derive the equations of motion for the system. The resulting Lagrange's equations are solved approximately and numerically using MAPLE software.

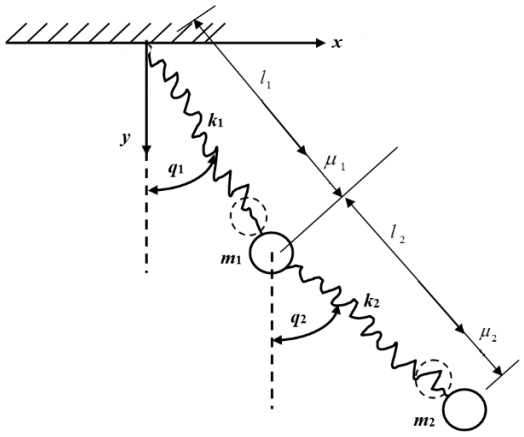

Fig. 1. Schematic diagram of a double spring-pendulum

2 Derivation of the Lagrange's equations of motion

Suppose the positions of mass m_1 and m_2 at any time in space is expressed in Cartesian coordinates as (x_1, y_1) and (x_2, y_2), unstretched lengths of the

springs are l_1 and l_2, and the springs extend by $\mu_1(t)$ and $\mu_2(t)$ when the respective masses are attached as shown in Figure 1.

At the point of suspension, the positions of the bobs are given by the following equations:

$$x_1(t) = (l_1 + \mu_1(t))\sin q_1(t) \tag{1}$$

$$y_1(t) = -(l_1 + \mu_1(t))\cos q_1(t) \tag{2}$$

$$x_2(t) = (l_1 + \mu_1(t))\sin q_1(t) + (l_2 + \mu_2(t))\sin q_2(t) \tag{3}$$

$$y_2(t) = -(l_1 + \mu_1(t))\cos q_1(t) - (l_2 + \mu_2(t))\cos q_2(t) \tag{4}$$

The total kinetic energy (T) of the system is given by:

$$T = \frac{1}{2}m_1\left(\dot{x}_1^2(t) + \dot{y}_1^2(t)\right) + \frac{1}{2}m_2\left(\dot{x}_2^2(t) + \dot{y}_2^2(t)\right) \tag{5}$$

$$\begin{aligned} T(q,\mu,\dot{q},\dot{\mu}) = {} & \frac{1}{2}m_1\left\{\dot{\mu}_1^2(t) + (l_1 + \mu_1(t))^2\dot{q}_1^2(t)\right\} + \\ & \frac{1}{2}m_2\begin{Bmatrix} \dot{\mu}_1^2(t) + \dot{\mu}_2^2(t) + (l_1 + \mu_1(t))^2\dot{q}_1^2(t) + (l_2 + \mu_2(t))^2\dot{q}_2^2(t) \\ + \left(2\dot{\mu}_1(t)\dot{\mu}_2(t) + 2(l_1 + \mu_1(t))(l_2 + \mu_2(t)\dot{q}_1(t)\dot{q}_2(t)\right)\cos(q_1 - q_2) \\ + \left(2(l_2 + \mu_2(t)\dot{\mu}_1(t)\dot{q}_2(t) - 2(l_1 + \mu_1(t)\dot{\mu}_2(t)\dot{q}_1(t)\right)\sin(q_1 - q_2) \end{Bmatrix} \end{aligned} \tag{6}$$

By taking a plane at distance (l_1+l_2) below the point of suspension of Figure 1 as a reference level, the potential (V) energy of the system is then given by:

$$\begin{aligned} V(q,\mu) = {} & m_1 g\left\{l_1 + l_2 - (l_1 + \mu_1(t))\cos q_1(t)\right\} + \\ & m_2 g\left\{l_1 + l_2 - (l_1 + \mu_1(t))\cos q_1(t) - (l_2 + \mu_2(t))\cos q_2(t)\right\} + \\ & \frac{1}{2}k_1\mu_1^2(t) + \frac{1}{2}k_2\mu_2^2(t) \end{aligned} \tag{7}$$

From this, the Lagrangian function for the system is given by:

$$L = T - V$$

$$\begin{aligned} L(q,\mu,\dot{\mu},\dot{q}) = {} & \frac{1}{2}m_1\left\{\dot{\mu}_1^2(t) + (l_1 + \mu_1(t))^2\dot{q}_1^2(t)\right\} + \frac{1}{2}m_2\left\{\dot{\mu}_1^2(t) + \dot{\mu}_2^2(t) + (l_1 + \mu_1(t))^2\dot{q}_1^2(t)\right. \\ & + (l_2 + \mu_2(t))^2\dot{q}_2^2(t) + \left(2\dot{\mu}_1(t)\dot{\mu}_2(t) + 2(l_1 + \mu_1(t))(l_2 + \mu_2(t)\dot{q}_1(t)\dot{q}_2(t)\right)\cos(q_1 - q_2) \\ & \left. + \left(2(l_2 + \mu_2(t)\dot{\mu}_1(t)\dot{q}_2(t) - 2(l_1 + \mu_1(t)\dot{\mu}_2(t)\dot{q}_1(t)\right)\sin(q_1 - q_2)\right\} \\ & - m_1 g\left\{l_1 + l_2 - (l_1 + \mu_1(t))\cos q_1(t)\right\} - m_2 g\left\{l_1 + l_2 - (l_1 + \mu_1(t))\cos q_1(t)\right. \\ & \left. -(l_2 + \mu_2(t))\cos q_2(t)\right\} + \frac{1}{2}k_1\mu_1^2(t) + \frac{1}{2}k_2\mu_2^2(t) \end{aligned} \tag{8}$$

The Lagrange's equations (Murray 1967, Goldstein *et al.* 2000, Martin and Salomonson 2009) associated with the generalized coordinates $q_1(t)$, $q_2(t)$, $\mu_1(t)$, and $\mu_2(t)$ are given by:

$$\begin{aligned} &\frac{d}{dt}\left(\frac{\partial L}{\partial \dot{q}_1}\right)-\left(\frac{\partial L}{\partial q_1}\right)=0, \qquad \frac{d}{dt}\left(\frac{\partial L}{\partial \dot{q}_2}\right)-\left(\frac{\partial L}{\partial q_2}\right)=0, \\ &\frac{d}{dt}\left(\frac{\partial L}{\partial \dot{\mu}_1}\right)-\left(\frac{\partial L}{\partial \mu_1}\right)=0, \qquad \frac{d}{dt}\left(\frac{\partial L}{\partial \dot{\mu}_2}\right)-\left(\frac{\partial L}{\partial \mu_2}\right)=0\ . \end{aligned} \tag{9}$$

Now differentiating equation (8) accordingly, and substituting into equation (9) gives four Lagrange's equations of motion for the system; one equation for each degree of freedom (i.e., q_1, q_2, μ_1 and μ_2). They are as follows:

$$\begin{aligned} &(m_1+m_2)(l_1+\mu_1(t))\ddot{q}_1(t)+m_2(l_2+\mu_2(t))\cos(q_1-q_2)\ddot{q}_2(t)-m_2\sin(q_1-q_2)\ddot{\mu}_2(t) \\ &\quad=-2(m_1+m_2)(l_1+\mu_1(t))\dot{\mu}_1(t)\dot{q}_1(t)-m_2(l_2+\mu_2(t))\sin(q_1-q_2)\dot{q}_1^2(t) \\ &\quad\quad-2m_2\cos(q_1-q_2)\dot{\mu}_2(t)\dot{q}_2(t)-\left(m_1+m_2\right)g\sin q_1 \end{aligned} \tag{10}$$

$$\begin{aligned} &m_2(l_2+\mu_2(t))\ddot{q}_2(t)+m_2\sin(q_1-q_2)\ddot{\mu}_1(t) \\ &\quad=-2m_2\cos(q_1-q_2)\dot{\mu}_1(t)\dot{q}_1(t)+m_2(l_1+\mu_1(t)\sin(q_1-q_2)\dot{q}_1^2(t) \\ &\quad\quad-2m_2(l_2+\mu_2(t))\dot{\mu}_2(t)\dot{q}_2(t)-m_2g\sin q_2 \end{aligned} \tag{11}$$

$$\begin{aligned} &m_2\left(l_2+\mu_2(t)\right)\sin(q_1-q_2)\ddot{q}_2(t)+\left(m_1+m_2\right)\ddot{\mu}_1(t)+m_2\cos(q_1-q_2)\ddot{\mu}_2(t) \\ &\quad=-2m_2\sin(q_1-q_2)\dot{\mu}_2(t)\dot{q}_2(t)+\left(m_1+m_2\right)\left(l_1+\mu_1(t)\right)\dot{q}_1^2(t) \\ &\quad\quad+m_2\left(l_2+\mu_2(t)\right)\left(1+\cos(q_1-q_2)\right)\dot{q}_2^2(t)+m_1g\left(\cos q_1+\cos q_2\right)-k_1\mu_1(t) \end{aligned} \tag{12}$$

$$\begin{aligned} &-m_2\left(l_1+\mu_1(t)\right)\sin(q_1-q_2)\ddot{q}_1(t)+m_2\cos(q_1-q_2)\ddot{\mu}_1(t)+m_2\ddot{\mu}_2(t) \\ &\quad=2m_2\sin(q_1-q_2)\dot{\mu}_1(t)\dot{q}_1(t)-m_2\left(\left(l_2+\mu_2(t)\right)-\left(l_1+\mu_1(t)\right)\cos(q_1-q_2)\right)\dot{q}_1^2(t) \\ &\quad\quad+m_2g\cos q_2-k_2\mu_2(t) \end{aligned} \tag{13}$$

Equations (10) – (13) represent a pair of coupled second order differential equations describing the unconstrained motion of a double spring-pendulum.

Generally, equations of motion can be represented in matrix form as:

$$M\ddot{p}(t)+c_1\dot{p}(t)+c_2p(t)=f(t) \tag{14}$$

Where, c_1 and c_2 are the damping coefficient and stiffness matrices. Rearranging equation (14), one obtains the mass matrix M and rest matrix R in the representation given by equation (15):

$$M\ddot{p}(t)=R(t) \tag{15}$$

where:

$$\ddot{p}(t) = M^{-1}R(t) \tag{16}$$

and

$$\ddot{p}(t) = \begin{pmatrix} \ddot{q}_1 \\ \ddot{q}_2 \\ \ddot{\mu}_1 \\ \ddot{\mu}_2 \end{pmatrix} \tag{17}$$

Substituting equations (10), (11), (12) and (13) into (15), we obtain

$$M = \begin{pmatrix} (m_1+m_2)(l_1+\mu_1(t)) & m_2(l_2+\mu_2(t))\cos(q_1-q_2) & 0 & -m_2\sin(q_1-q_2) \\ 0 & m_2(l_2+\mu_2(t)) & m_2\sin(q_1-q_2) & 0 \\ 0 & m_2\left(l_2+\mu_2(t)\right)\sin(q_1-q_2) & \left(m_1+m_2\right) & m_2\cos(q_1-q_2) \\ -m_2\left(l_1+\mu_1(t)\right)\sin(q_1-q_2) & 0 & m_2\cos(q_1-q_2) & m_2 \end{pmatrix} \tag{18}$$

$$\ddot{p}(t) = \begin{pmatrix} \ddot{q}_1 \\ \ddot{q}_2 \\ \ddot{\mu}_1 \\ \ddot{\mu}_2 \end{pmatrix} \tag{19}$$

$$R = \begin{pmatrix} -2(m_1+m_2)(l_1+\mu_1(t))\dot{\mu}_1(t)\dot{q}_1(t) - m_2(l_2+\mu_2(t))\sin(q_1-q_2)\dot{q}_1^2(t) - 2m_2\cos(q_1-q_2)\dot{\mu}_2(t)\dot{q}_2(t) \\ -\left(m_1+m_2\right)g\sin q_1 \\ -2m_2\cos(q_1-q_2)\dot{\mu}_1(t)\dot{q}_1(t) + m_2(l_1+\mu_1(t)\sin(q_1-q_2)\dot{q}_1^2(t) - 2m_2(l_2+\mu_2(t))\dot{\mu}_2(t)\dot{q}_2(t) \\ -m_2 g\sin q_2 \\ -2m_2\sin(q_1-q_2)\dot{\mu}_2(t)\dot{q}_2(t) + \left(m_1+m_2\right)\left(l_1+\mu_1(t)\right)\dot{q}_1^2(t) + m_2\left(l_2+\mu_2(t)\right)\left(1+\cos(q_1-q_2)\right)\dot{q}_2^2(t) \\ +m_1 g\left(\cos q_1+\cos q_2\right) - k_1\mu_1(t) \\ 2m_2\sin(q_1-q_2)\dot{\mu}_1(t)\dot{q}_1(t) - m_2\left(\left(l_2+\mu_2(t)\right)-\left(l_1+\mu_1(t)\right)\cos(q_1-q_2)\right)\dot{q}_1^2(t) + m_2 g\cos q_2 - k_2\mu_2(t) \end{pmatrix} \tag{20}$$

The matrix equations in (18), (19) and (20) represent a four dimensional system of equations of motion for the double spring-pendulum in generalized coordinates: q_1, q_2, μ_1 and μ_2. The size of the mass matrix *M* is 4 x 4 and that of the rest matrix *R* is 4 x 1.

The coupled second order differential equations can only be solved approximately (Murray, 1967). Considering a case where

$m_1 = m_2 = m,\ \mu_1 = \mu_2 = \mu,\ l_1 = l_2 = l$ and $k_1 = k_2,$ these equations simplifies to the following:

$$\begin{aligned} &2(l+\mu(t))\ddot{q}_1(t) + (l+\mu(t))\cos(q_1-q_2)\ddot{q}_2(t) - \sin(q_1-q_2)\ddot{\mu}_2(t) \\ &= -4(l+\mu(t))\dot{\mu}_1(t)\dot{q}_1(t) - (l_2+\mu_2(t))\sin(q_1-q_2)\dot{q}_1^2(t) - 2\cos(q_1-q_2)\dot{\mu}_2(t)\dot{q}_2(t) - 2g\sin q_1 \end{aligned} \tag{21}$$

$$\begin{aligned} &(l+\mu(t))\ddot{q}_2(t) + \sin(q_1-q_2)\ddot{\mu}_1(t) \\ &= -2\cos(q_1-q_2)\dot{\mu}_1(t)\dot{q}_1(t) + (l+\mu(t)\sin(q_1-q_2)\dot{q}_1^2(t) - 2(l+\mu(t))\dot{\mu}_2(t)\dot{q}_2(t) - g\sin q_2 \end{aligned} \tag{22}$$

$$\begin{aligned} &\big(l+\mu(t)\big)\sin(q_1-q_2)\ddot{q}_2(t) + 2\ddot{\mu}_1(t) + \cos(q_1-q_2)\ddot{\mu}_2(t) + 2\sin(q_1-q_2)\dot{\mu}_2(t)\dot{q}_2(t) \\ &= 2\big(l+\mu(t)\big)\dot{q}_1^2(t) + \big(l+\mu(t)\big)\big(1+\cos(q_1-q_2)\big)\dot{q}_2^2(t) + g\left(\cos q_1 + \cos q_2\right) - \frac{k}{m}\mu(t) \end{aligned} \tag{23}$$

$$\begin{aligned} &-\big(l+\mu(t)\big)\sin(q_1-q_2)\ddot{q}_1(t) + \cos(q_1-q_2)\ddot{\mu}_1(t) + \ddot{\mu}_2(t) \\ &= 2\sin(q_1-q_2)\dot{\mu}_1(t)\dot{q}_1(t) - \Big(\big(l+\mu(t)\big) - \big(l+\mu(t)\big)\cos(q_1-q_2)\Big)\dot{q}_1^2(t) + g\cos q_2 - \frac{k}{m}\mu(t) \end{aligned} \tag{24}$$

These equations can be solved exactly for small angle of deflection. For small oscillations, we use the approximations:

$\sin(q_1-q_2) \approx q_1 - q_2,\ \cos(q_1-q_2) \approx 1,$ and neglecting terms involving $\dot{\mu}\dot{q},\ \dot{q}^2$, in equations (21) – (24), we get

$$2(l+\mu(t))\ddot{q}_1(t) + (l+\mu(t))\ddot{q}_2(t) - (q_1-q_2)\ddot{\mu}_2(t) = -2gq_1 \tag{25}$$

$$(l+\mu(t))\ddot{q}_2(t) + (q_1-q_2)\ddot{\mu}_1(t) = -gq_2 \tag{26}$$

$$\big(l+\mu(t)\big)(q_1-q_2)\ddot{q}_2(t) + 2\ddot{\mu}_1(t) + \ddot{\mu}_2(t) = 2g - \frac{k}{m}\mu(t) \tag{27}$$

$$-\big(l+\mu(t)\big)(q_1-q_2)\ddot{q}_1(t) + \ddot{\mu}_1(t) + \ddot{\mu}_2(t) = g - \frac{k}{m}\mu(t) \tag{28}$$

From equations (25) and (26), we have that:

$$\begin{aligned} \ddot{\mu}_1(t) &= \frac{-1}{(q_1-q_2)}\left\{(l+\mu(t))\ddot{q}_2(t) + gq_2\right\} \\ \ddot{\mu}_2(t) &= \frac{1}{(q_1-q_2)}\left\{2(l+\mu(t))\ddot{q}_1(t) + (l+\mu(t))\ddot{q}_2(t) + 2gq_1\right\} \end{aligned} \tag{29}$$

Substituting equation (29) into equations (27) and (28), and neglecting terms involving $q_1q_2,\ q^2,\ \left(q_1-q_2\right)^2$, we get

$$2\left(l+\mu(t)\right)\ddot{q}_1(t)-\left(l+\mu(t)\right)\ddot{q}_2(t)=-\frac{k}{m}\mu(t)(q_1-q_2) \tag{30}$$

$$2\left(l+\mu(t)\right)\ddot{q}_1(t)=-gq_1-\frac{k}{m}\mu(t)(q_1-q_2) \tag{31}$$

The normal frequencies and normal modes that correspond to small oscillations for the double spring-pendulum is calculated from equations (30) and (31) by using equation (32)

$$q_1=A_1e^{i\omega t},\quad q_2=A_2e^{i\omega t}. \tag{32}$$

Substituting the derivatives of (32) into (30) and (31), and simplifying gives

$$\left(2\left(l+\mu(t)\right)\omega^2-\frac{k}{m}\mu(t)\right)A_1-\left(\left(l+\mu(t)\right)\omega^2-\frac{k}{m}\mu(t)\right)A_2=0 \tag{33}$$

$$\left(2\left(l+\mu(t)\right)\omega^2-\left(g+\frac{k}{m}\mu(t)\right)\right)A_1+\frac{k}{m}\mu(t)A_2=0 \tag{34}$$

In order for A_1 and A_2 to be non-zero, we must set the determinant of the coefficients equal to zero. That is,

$$\begin{vmatrix} 2\left(l+\mu(t)\right)\omega^2-\frac{k}{m}\mu(t) & -\left(\left(l+\mu(t)\right)\omega^2-\frac{k}{m}\mu(t)\right) \\ 2\left(l+\mu(t)\right)\omega^2-\left(g+\frac{k}{m}\mu(t)\right) & \frac{k}{m}\mu(t) \end{vmatrix}=0 \tag{35}$$

or $2\left(l+\mu\right)^2\omega^4-\left(l+\mu\right)\left(g+\frac{k}{m}\mu\right)\omega^2+g\frac{k}{m}\mu=0$. On solving this equation, we get

$$\omega^2=\frac{\left(g+\frac{k}{m}\mu\right)\pm\sqrt{\left(g+\frac{k}{m}\mu\right)^2-8g\frac{k}{m}\mu}}{4(l+\mu)} \tag{36}$$

Using the positive and negative parts of ω^2 in equation (36), the normal frequencies are given by

$$f_1=\frac{\omega_1}{2\pi}=\frac{1}{2\pi}\left(\frac{\left(g+\frac{k}{m}\mu\right)+\sqrt{\left(g+\frac{k}{m}\mu\right)^2-8g\frac{k}{m}\mu}}{4(l+\mu)}\right)^{\frac{1}{2}}, \tag{37}$$

and

$$f_2 = \frac{\omega_2}{2\pi} = \frac{1}{2\pi}\left(\frac{\left(g + \frac{k}{m}\mu\right) - \sqrt{\left(g + \frac{k}{m}\mu\right)^2 - 8g\frac{k}{m}\mu}}{4(l+\mu)} \right)^{\frac{1}{2}} \tag{38}$$

Substituting the positive part of equation (36) into equation (34) gives

$$A_1 = \frac{-\frac{k}{m}\mu}{-\left(g + \frac{k}{m}\mu\right) + \sqrt{\left(g + \frac{k}{m}\mu\right)^2 - 8g\frac{k}{m}\mu}} A_2 \tag{39}$$

Equation (39) corresponds to the normal mode in which the bobs of mass m_1 and m_2 are moving in opposite directions. This is called the anti-symmetric mode.

Also, substituting the negative part of equation (36) into equation (34) gives

$$A_1 = \frac{\frac{k}{m}\mu}{\left(g + \frac{k}{m}\mu\right) + \sqrt{\left(g + \frac{k}{m}\mu\right)^2 - 8g\frac{k}{m}\mu}} A_2 \tag{40}$$

This corresponds to the normal mode in which the bobs are moving in the same directions.

3 Numerical solution

Maple software (Maple, 2018) is used to numerically solve the set of second order differential equations given by the Lagrange's equations of motion. In order to perform numerical analysis for the system, first the position coordinates (x_1, y_1, x_2, y_2) are defined. Thereafter, Maple performs the following tasks for the system:

- Calculates time derivatives ($\dot{x}_1$, $\dot{y}_1$, $\dot{x}_2$, $\dot{y}_2$) of the position coordinates.
- Evaluates kinetic energy for the system.
- Evaluates potential energy for the system with reference to distance below the point of suspension.
- Obtains the Lagrangian function from the difference between kinetic and potential energies.

- Evaluates the derivatives:
  $\frac{\partial L}{\partial q_1}, \frac{\partial L}{\partial q_2}, \frac{\partial L}{\partial \mu_1}, \frac{\partial L}{\partial \mu_2}, \frac{\partial L}{\partial \dot{q}_1}, \frac{\partial L}{\partial \dot{q}_2}, \frac{\partial L}{\partial \dot{\mu}_1}, \frac{\partial L}{\partial \dot{\mu}_2}$.
- Calculates the Lagrange's equations associated with the generalized coordinates q_1, q_2, μ_1, μ_2.
- Numerically solves the Lagrange's equations associated with q_1, q_2, μ_1, μ_2 for different values of m_1, m_2, g, k_1, k_2, L_1 and L_2.

New parameters (X_1, Y_1, X_2, Y_2) were defined to calculate the positions of the two masses m_1 and m_2 in the *xy* plane.

Finally, the software evaluates these new parameters and the results are used to plot variation in position of pendulum bobs (m_1 and m_2) with respect to time along the *x*- and *y*-axis, respectively.

Due to space constraints, the Maple commands are not displayed here but can be viewed as supplementary files attached to this article. Only motions of the pendulum bobs (m_1 and m_2) are displayed in Fig. 2 for $g = 9.8$, $k_1 = k_2 = 0.01$, $L_1 = L_2 = 0.5$, $m_1 = m_2 = 0.1$, $q_1 = q_2 = 1$, $\mu_1 = \mu_2 = 0.05$.

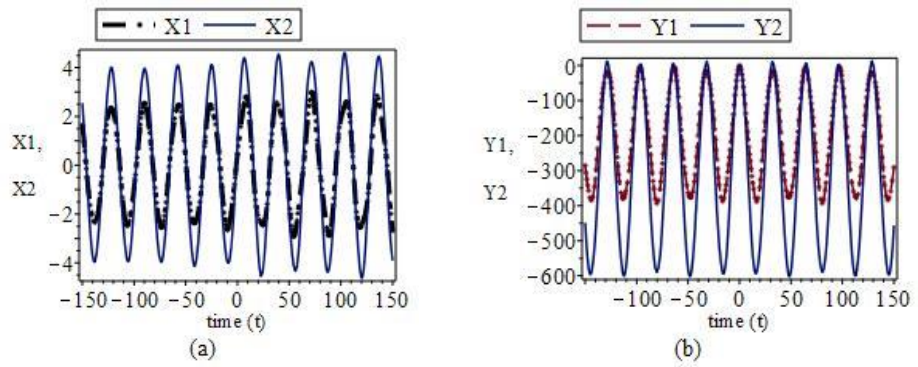

Fig. 2. Comparison between the motions of mass m_1 and m_2 along the (a) horizontal and (b) vertical planes.

Figure 2 represents variation in position of the pendulum bobs m_1 and m_2 with respect to time along the *x*- and *y*-axis. The plots show sinusoidal curves that are continuous and periodic with slightly changing amplitudes. Figure 2(a) is characteristics of a sine wave function while Figure 2(b) is characteristics of a cosine wave function. The slightly varying amplitudes observed in the curves might be as a result of the chaotic nature of single and double spring-pendulum. Figure 2 shows comparison of the motion of pendulum bob m_1 and m_2. It is observed that the amplitudes of the curves representing motion for m_1 are smaller than those of motion for m_2 as displayed by Figures 2(a) and 2(b), respectively.

Furthermore, we studied the behaviour of the pendulum bobs for: $k_1 \neq k_2$, $q_1 \neq q_2$, $m_1 \neq m_2$, and $L_1 \neq L_2$. For $k_2 > k_1$, curves representing the motion of the pendulum bobs are shown in Figures 3(a) and (b). When k_1 is fixed at 0.01, and the stiffness constant of the second spring (k_2) is increased from 0.05 to 1, we observed that the two bobs are in phase, periodic and the amplitudes are suppressed as displayed in Figures 3(a) and (b). This is an indication of a non-chaotic regime. Furthermore, the wave forms of the two bobs along the *x*-plane (X1, X2, X3, X4, X5 and X6) are seen to diverge as they progress with time.

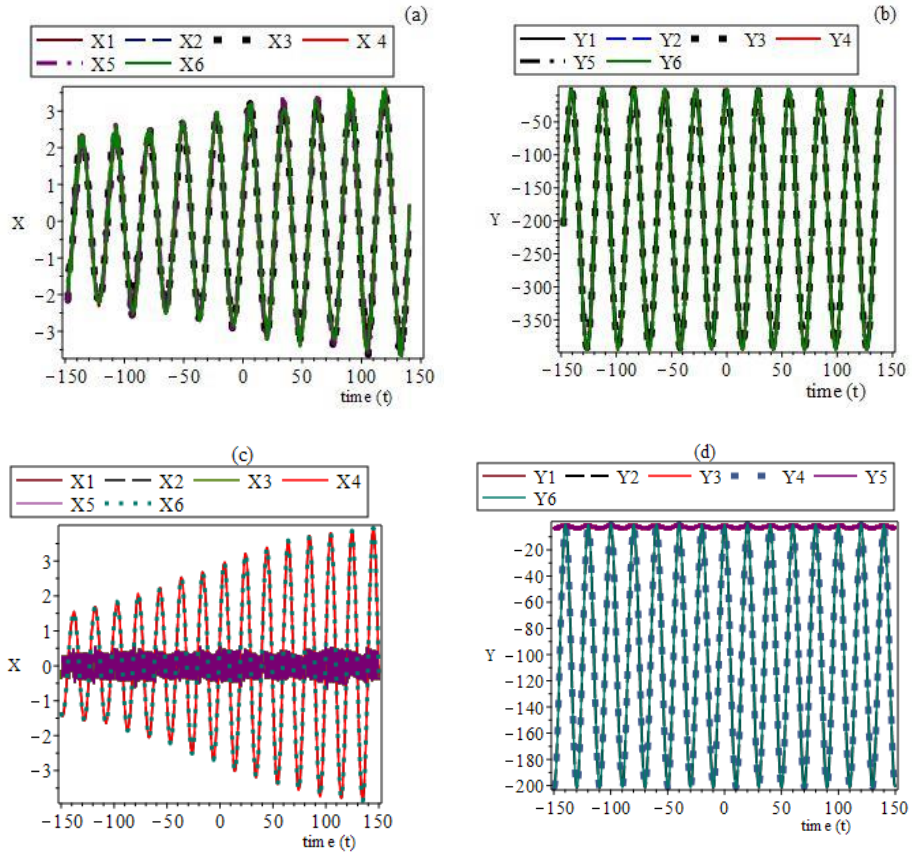

Fig. 3. Motion of inner and outer bob along the horizontal and vertical planes for $g = 9.8, L_1 = L_2 = 0.5, m_1 = m_2 = 0.1, q_1 = q_2$=1 and $\mu_1 = \mu_2 = 0.05$ where (a) and (b) for $k_2 > k_1$, and (c) and (d) for $k_1 > k_2$.

In Figures 3(a & b): X1, X2, Y1 and Y2 represent motions of pendulum bob (1&2) along the *x*- and *y*-plane for $k_1 = 0.01$ and $k_2 = 0.05$. X3, X4, Y3 and Y4 represent motions of bobs along the *x*- and *y*-plan for $k_1 = 0.01$ and $k_2 = 0.5$, and X5, X6, Y5 and Y6 represent motions of bobs along the *x*- and *y*-

plane for $k_1 = 0.01$ and $k_2 = 1$. In Figures 3(c & d): X1, X2, Y1 and Y2 represent motions of pendulum bobs for $k_1 = 0.05$ and $k_2 = 0.01$. X3, X4, Y3 and Y4 represent motions of bobs for $k_1 = 0.5$ and $k_2 = 0.01$, and X5, X6, Y5 and Y6 represent motions of bobs for $k_1 = 1$ and $k_2 = 0.01$.

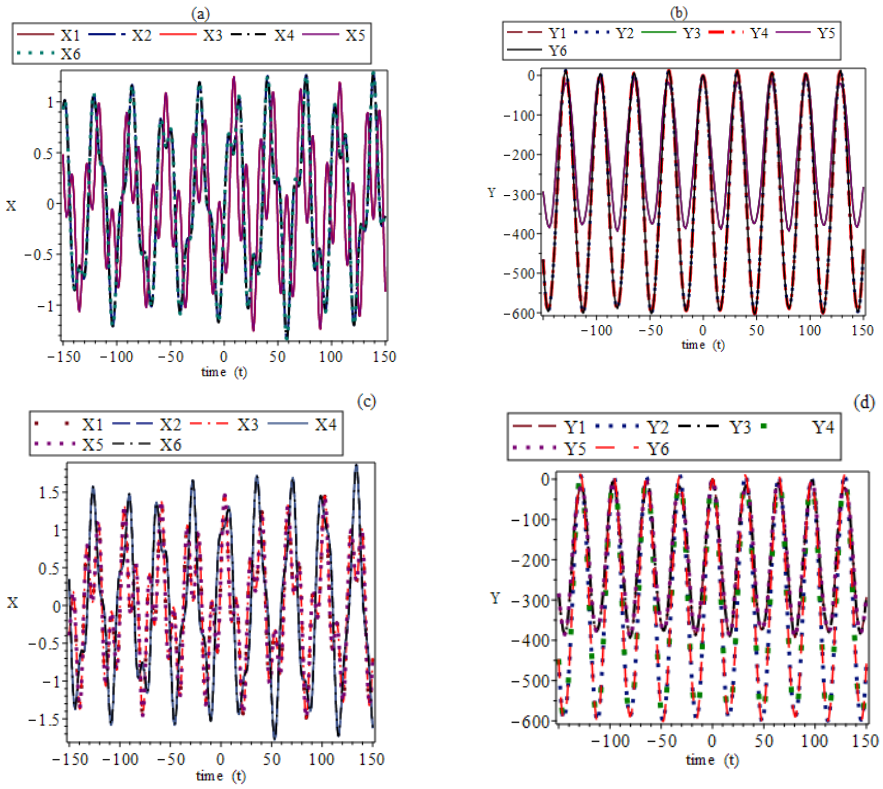

Fig. 4. Motion of the inner and outer bob along the horizontal and vertical planes for $g = 9.8, L_1 = L_2 = 0.5, m_1 = m_2 = 0.1, k_1 = k_2 = 0.01$ and $\mu_1 = \mu_2 = 0.05$ where (a) and (b) for $q_1 > q_2$, and (c) and (d) for $q_2 > q_1$.

For $k_1 > k_2$, the motions of the bobs are displayed in Figures 3(c & d). As the stiffness constant of the first spring k_1 is increased from 0.05 to 1 with k_2 fixed at 0.01, we entered a non-periodic regime. This can be likened to increase in energy that gives rise to quasi-periodic regime as reported by Biglari and Jami (2016). This is clearly seen in the curves associated with the motion of the inner bob m_1 along both x and y planes as shown in Figures 3(c & d). However, we observed that for the curves representing the outer pendulum bob m_2 along the vertical plane are periodic with negative values.

Also, keeping the angle of displacement q_2 fixed at 1, and increasing q_1 (=3, 4.5, 4.7), we observed a chaotic behaviour and as well the amplitudes are suppressed as shown in Figure 4(a). While for curves representing positions of the inner and outer bobs along the *y* plane show only slight variation in amplitude (see Figure 4(b)).

In Figures 4(a & b): X1, X2, Y1 and Y2 represent motions of pendulum bob (1&2) along the *x*- and *y*-plane for $q_1 = 3$ and $q_2 = 1$. X3, X4, Y3 and Y4 represent motions of bobs along the *x*- and *y*-plane for $q_1 = 4.5$ and $q_2 = 1$, and X5, X6, Y5 and Y6 represent motions of bobs along the *x*- and *y*-plane for $q_1 = 4.7$ and $q_2 = 1$. In (c & d): X1, X2, Y1 and Y2 represent motions of pendulum bobs for $q_1 = 1$ and $q_2 = 0.5$. X3, X4, Y3 and Y4 represent motions of bobs for $q_1 = 1$ and $q_2 = 1.5$, and X5, X6, Y5 and Y6 represent motions of bobs for $q_1 = 1$ and $q_2 = 2$.

Increasing q_2 (= 0.5, 1.5, 2) with q_1 fixed, we noticed the two bobs do not move together, amplitudes of the graphs are suppressed and there exist quasi-periodic behaviour indicating a chaotic regime as displayed in Figure 4(c). In addition, when the mass of the outer pendulum bob m_2 is fixed at 0.05 and m_1 is increased from 0.1 to 2, we noticed from Figure 5(a) that the two bobs do not move together along the *x* plane. Again this indicates the presence of chaos; as such X1, X2, X3, X4, X5 and X6 are out of phase. But, in Figure 5(b) the two bobs are in phase and periodic along the *y* plane. Also, we observed that the amplitudes of the graphs have a tendency to increase with mass. On the other hand, when m_1 is fixed and m_2 is varied, one noticed from Figures (c & d), that the bobs move together along both axes. Nevertheless, there are indications of the presence of chaos on the graphs X1, X3, X5 and X7 as m_2 is increased from 0.1 to 2.

In Figures 5 (a & b): X1, X2, Y1 and Y2 represent motions of pendulum bob (1&2) along the *x*- and *y*-plane for $m_1 = 0.1$ and $m_2 = 0.05$. X3, X4, Y3 and Y4 represent motions of bobs along the *x*- and *y*-plane for $m_1 = 0.5$ and $m_2 = 0.05$, and X5, X6, Y5 and Y6 represent motions of bobs along the *x*- and *y*-plane for $m_1 = 1$ and $m_2 = 0.05$. X7, X8, Y7 and Y8 represent curves for bobs along the *x*- and *y*-plane for $m_1 = 2$ and $m_2 = 0.05$. In (c & d): X1, X2, Y1 and Y2 represent curves for pendulum bobs along the *x*- and *y*-plane for $m_1 = 0.05$ and $m_2 = 0.1$. X3, X4, Y3 and Y4 represent curves for bobs along the *x*- and *y*-plane for $m_1 = 0.05$ and $m_2 = 0.5$. X5, X6, Y5 and Y6 represent curves for bobs along the *x*- and *y*-plane for $m_1 = 0.05$ and $m_2 = 1$, and X7, X8, Y7 and Y8 represent curves for bobs along the *x*- and *y*-plane for $m_1 = 0.05$ and $m_2 = 2$.

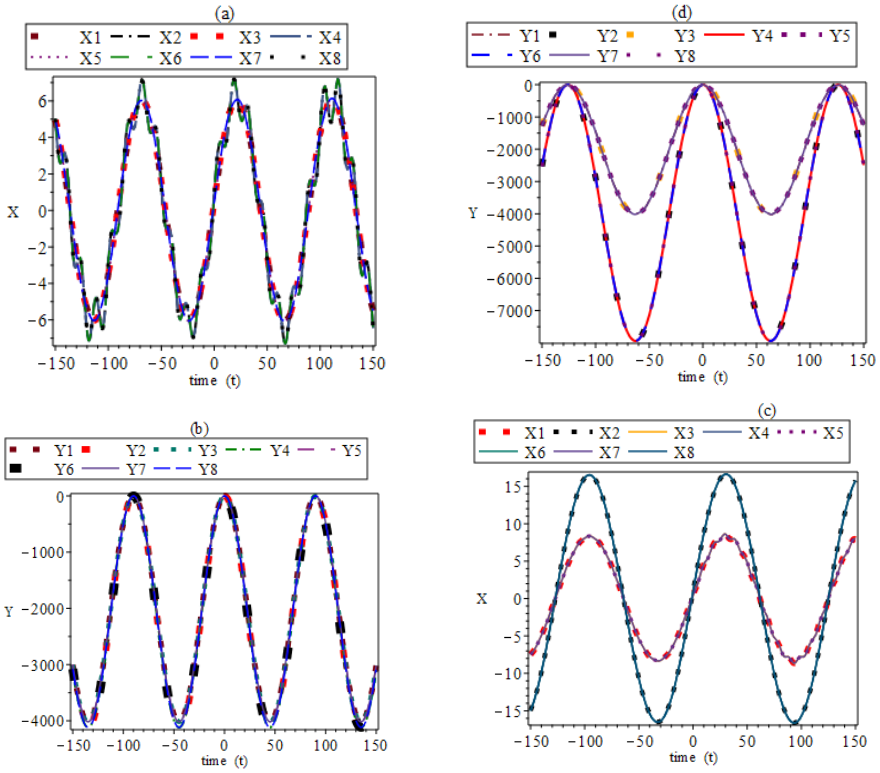

Fig. 5. Motion of the inner and outer bob along the horizontal and vertical planes for $g = 9.8, L_1 = L_2 = 0.5, q_1 = q_2 = 1, k_1 = k_2 = 0.01$ and $\mu_1 = \mu_2 = 0.05$ **where (a) and (b) for** $m_1 > m_2$, and **(c) and (d) for** $m_2 > m_1$.

Finally, increasing the length of the inner or outer spring has significant effect on the motion of the pendulum bobs. Keeping L_1 fixed and increasing the length of the outer spring L_2, or keeping L_2 fixed and increasing the length of the inner spring L_1, we observed that the inner and outer pendulum bobs do not move together along the x plane as shown in Figures 6 (a & c). Hence, signifies the existence of a chaotic regime. On the other hand, along the y plane the two bobs are in phase and periodic showing there is no chaos along this plane. This periodic and chaotic behaviour is consistent with previous studies on spring-pendulum systems (Lewin and Chen 2015, Carretero-Gonzalez *et al.* 1994, Leah 2013, Nunez-Yepez *et al.* 1990).

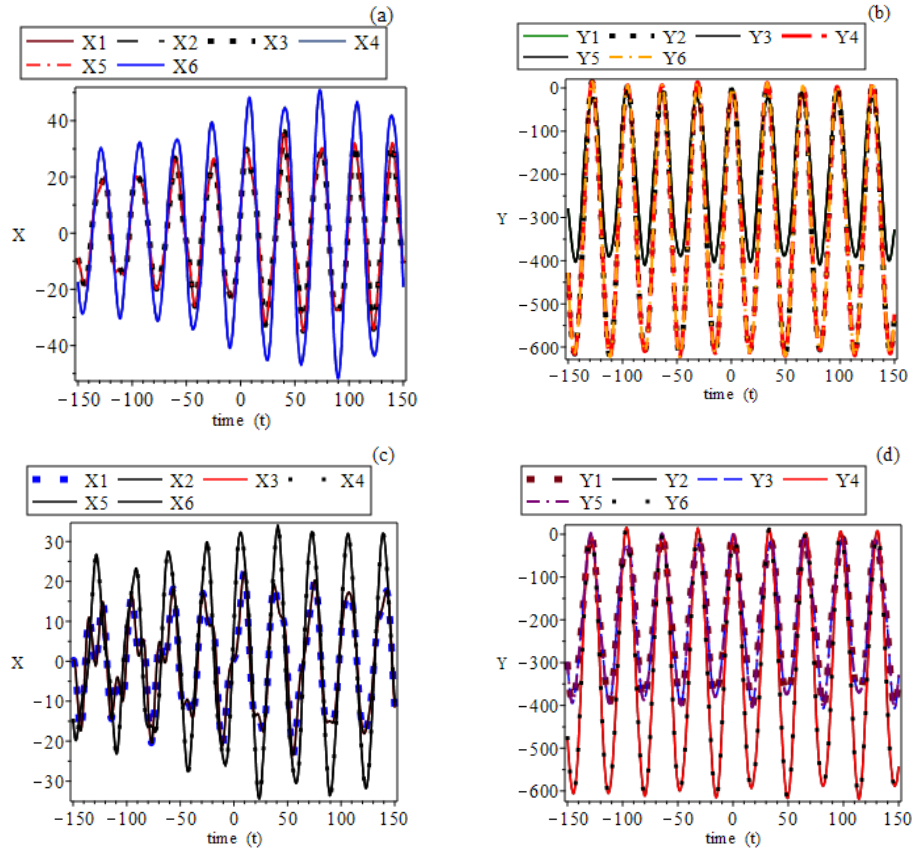

Fig. 6. Motion of the inner and outer bob along the horizontal and vertical planes for $g = 9.8, m_1 = m_2 = 0.1, q_1 = q_2 = 1, k_1 = k_2 = 0.01$ and $\mu_1 = \mu_2 = 0.05$ where (a) and (b) $L_1 > L_2$, , and (c) and (d) $L_2 > L_1$.

In Figures 6 (a & b): X1, X2, Y1 and Y2 represent motions of pendulum bobs (1&2) along the *x*- and *y*-plane for $L_1 = 2$ and $L_2 = 0.5$. X3, X4, Y3 and Y4 represent motions of bobs along the *x*- and *y*-plane for $L_1 = 5$ and $L_2 = 0.5$, and X5, X6, Y5 and Y6 represent motions of bobs along the *x*- and *y*-plane for $L_1 = 10$ and $L_2 = 0.5$. In (c & d): X1, X2, Y1 and Y2 represent motions of pendulum bobs for $L_1 = 0.5$ and $L_2 = 2$. X3, X4, Y3 and Y4 represent motions of bobs for $L_1 = 0.5$ and $L_2 = 5$, and X5, X6, Y5 and Y6 represent motions of bobs for $L_1 = 0.5$ and $L_2 = 10$.

4 Conclusions

Equations of motion for the 2D double spring-pendulum with time dependent spring extension are derived using Lagrangian formulation of mechanics in generalized coordinates and are solved approximately. These equations were also solved numerically with Maple and it was observed that motion along the x-axis is characterized by a sine wave curve while motion along the y-axis is characterized by a cosine wave curve. Change in stiffness constant, angle of deflection, mass of pendulum bob and spring length were found to have significant effect on the dynamics of a 2D double spring-pendulum. The periodic and chaotic behaviour noticed in this study is consistent with current literature on spring-pendulum systems.

Acknowledgements

Comments from two anonymous RJS reviewers on the initial draft of the submitted manuscript are acknowledged.

References

Baleanu D, Asad, JH, Petras I. 2015. Numerical solution of the fractional Euler-Lagrange's equations of a thin elastic model. *Nonlinear Dynamics* 81: 97-102. https://doi.org/10.1007/s11071-015-1975-7

Biglari H, Jami RA. 2016. The double pendulum numerical analysis with Lagrangian and the Hamiltonian equations of motions. Conference paper: International conference on mechanical and aerospace engineering. pp 1-12. https://www.researchgate.net/publication/301890703

Carretero-Gonzalez R, Nunez-Yepez NH, Salas-Brito LA. 1994. Regular and chaotic behaviour in an extensible pendulum, *European Journal of Physics* 15: 139. https://doi.org/10.1088/0143-0807/15/3/009

de Sousa MC, Marcus FA, Caldas IL. 2017. Energy distribution in spring pendulum. *Nonlinear Optics* 4: 6.

Goldstein H, Poole C, Safko J. 2000. Classical mechanics, 3rd edn. Addison Wesley, New York, 5-69.

Leah G. 2013. The Swinging Spring: Regular and Chaotic Motion. http://depts.washington.edu/amath/wordpress/wp-content/uploads/2014/01/leah_ganis_pres.pdf

Lewin A, Chen P. 2015. Numerical analysis of dynamics of single and double spring pendulum systems. https://www.math.dartmouth.edu/~m53f15/proj/chenlewin.pdf

Maple 2018. Maplesoft, a division of Waterloo Maple Inc., Waterloo, Ontario.

Marcus FA, de Sousa MC, Caldas IL. 2016. Order-chaos-order transition in a spring pendulum, 6th International Conference on Nonlinear and Complexity, National Institute for Space Research, Brazil, May 16-20.

Martin C, Salomonson P. 2009. An introduction to analytical mechanics, 4th edn. Goteborg Sweden 1-62 pp.

Murray RS. 1967. Theoretical mechanics, Schaum's outlines, Mcgraw-Hill 299 – 301 pp.

Nunez-Yepez NH, Salas-Brito LA,Vicente L. 1990. Onset of Chaos in an Extensible Pendulum. *Physics Letters A* 145:101–105. https://doi.org/10.1016/0375-9601(90)90199-X

Smith RA. 2002. Numerical solution of equations of motion for double pendulum, Maple document Application center.1-5 pp.